Astron. Astrophys. 321, 765–770 (1997)

ASTRONOMY
AND
ASTROPHYSICS

The neutral gas content of X-ray bright elliptical galaxies

J. Braine[1], **C. Henkel**[2], **and T. Wiklind**[3]

[1] Institut de RadioAstronomie Millimétrique, 300 rue de la Piscine, F-38240 St. Martin d'Hères, France
[2] Max-Planck-Institut für Radioastronomie, Auf dem Hügel 69, D-53121 Bonn, Germany
[3] Onsala Space Observatory, S-43992 Onsala, Sweden

Received 16 August 1995 / Accepted 8 November 1996

Abstract. Sensitive CO observations are presented for a sample of elliptical galaxies which are luminous X-ray and weak far infrared (FIR) emitters. Only non-detections were obtained. The absence of detectable amounts of CO (this includes the previously 'detected' prototypical galaxy NGC 4472) does not support those standard cooling flow scenarios in which dust grain sputtering reduces the FIR luminosity, while cooled down gas is forming a significant mass of dense molecular gas.

Key words: galaxies: cooling flows – galaxies: individual, NGC 4472 – galaxies: ISM – galaxies: elliptical – radio lines: galaxies – X-rays: galaxies

1. Introduction

Early-type galaxies have long been considered to be essentially devoid of interstellar matter and star forming activity. The concept of gas-free inert stellar systems was based on the lack of visible tracers of interstellar gas and massive stars. It had to be given up when refined observational techniques showed that individual early-type galaxies possess tiny amounts of warm ionized gas ($10^2 - 10^4\,M_\odot$; e.g. Caldwell 1984; Phillips et al. 1986), moderate amounts of cool neutral gas ($\sim 10^7\,M_\odot$; e.g. Lees et al. 1991; Wiklind et al. 1995), and large amounts of hot coronal gas ($10^8 - 10^{10}\,M_\odot$; e.g. Sarazin 1990).

The global dynamics of the X-ray emitting coronal gas is controlled by the competition between heating and cooling processes. The cooling rate increases sharply with decreasing radius, which results in a growing imbalance between heating and cooling. For the same reasons as in clusters, although on a much smaller scale, a pressure-driven "cooling flow" is present in the absence of heating sources strong enough to maintain the pressure balance.

To reach the stellar stage, the cooling gas has to pass a neutral phase where HI and CO should be abundant. Like the intracluster gas, the gas in X-ray bright ellipticals is also relatively metal enriched ($0.3 - 0.5 Z_\odot$; e.g. Mushotsky et al. 1994). The column density thresholds for CO self-shielding and self-gravitation of a molecular cloud are similar (cf. Elmegreen 1985) and stars should form exclusively through molecular clouds. Some models of cluster cooling flows (Ferland et al. 1994) have suggested the H_2 forms efficiently *without* dust. While H_2 formation on grains is a much more rapid process in the ISM (Hill & Hollenbach 1976; Spitzer 1978), molecular hydrogen can also form via H^- in regions without dust grains. The efficiency depends chiefly on the ionization and neutral fractions (Hill & Hollenbach 1976). H_2 formation via H^- has been invoked by Lequeux & Viallefond (1980) for the extremely metal-poor galaxy IZw 18. Since dust should be destroyed in the hot halo gas (Draine & Salpeter 1979) unless protected, a correlation between molecular gas and dust mass as observed in the Galactic disk is not expected. So far early-type galaxy samples observed in CO have been selected according to their infrared properties. The inferred decoupling of CO and infrared luminosities (low $L_{\rm FIR}$ due to lack of dust) requires a different approach: The search for CO emission in early-type galaxies with a high cooling rate ($\dot{M}_{\rm X}$). Here we thus study CO emission in a sample of prominent X-ray emitting galaxies without strong far-infrared emission (see Table 1). We have deliberately avoided galaxies at the centers of clusters in this study. Previous searches for CO emission in reported cluster cooling flows have reached negative results (Grabelsky & Ulmer 1990; Braine & Wiklind 1993; Braine & Dupraz 1994; McNamara & Jaffe 1994; O'Dea et al. 1994) except for the Perseus cluster (Lazareff et al. 1989). No CO has been detected in absorption in any reported cooling flow, including Perseus A (Braine et al. 1995).

Four of the six galaxies in our sample are part of the Thomas et al. (1986) sample of elliptical galaxies. Based on X-ray data, they find "cooling flows" in their entire sample. We compare our results with theirs to assess whether hot gas is cooling into neutral gas.

2. Observations and data reduction

The observations were made during two runs in May/June and August 1994 with the IRAM 30-m telescope at Pico Veleta (Spain).

Send offprint requests to: Jonathan Braine

Table 1. Source list, coordinates, and basic fluxes

Source	RA(1950)	Dec(1950)	D Mpc	cz km s^{-1}	B_T^0 mag.	$S_{\rm X}$ see Notes	$S_{\rm HI}$	$S_{60\mu{\rm m}}$ mJy	$S_{100\mu{\rm m}}$ mJy
NGC 315, pgc 3455	00 55 05.9	+30 04 58	104	4936 ± 24	11.87		ND[a]	310 ± 51	400 ± 102
NGC 720, pgc 6983	01 50 34.4	−13 59 06	35	1716 ± 11	11.13	76.7 ± 8.3	ND	0 ± 41	0 ± 63
NGC 4365, pgc 40375	12 21 55.0	+07 35 43	20.4	1227 ± 13	10.42	23.6 ± 6.0	ND	0 ± 44	650 ± 131[c]
NGC 4406, pgc 40653	12 23 39.7	+13 13 25	20.4	-248 ± 11	9.71	438.2 ± 17.6	1.3[b]	110 ± 35[d]	330 ± 67
NGC 4472, pgc 41220	12 27 13.9	+08 16 32	20.4	983 ± 10	9.26	836.7 ± 19.7	ND	0 ± 65	0 ± 106
NGC 4636, pgc 42734	12 40 16.6	+02 57 43	18	927 ± 13	10.37	631.6 ± 37.3	ND	140 ± 42	0 ± 171

Notes to Table 1:

Velocities are optical from de Vaucouleurs et al. (1991; hereafter RC3); B_T^0 from RC3; all $(B-V)_T^0$ and $(U-B)_T^0$ colors (RC3) are within the ranges (0.90,0.96) and (0.43, 0.56) respectively. X-ray fluxes are from Roberts et al. (1991) in units of 10^{-14} erg s^{-1} cm^{-2}. IRAS data at 60μ and 100μ are from Knapp et al. (1989). *a*: HI detected in absorption (Heckman et al. 1983; Chamaraux et al. 1987). *b*: in Jy km s^{-1}, Bregman et al. (1988). *c*: Jura et al. (1987) find 0 ± 183; *d*: White et al. (1991) find 60μ emission offcenter.

Table 2. CO Observations and limits to $I_{\rm CO}$

Source	rms_{10} 1 MHz mK	rms_{10} 8 MHz mK	rms_{21} 1 MHz mK	rms_{21} 8 MHz mK	rms_{10}^a 8 MHz mK	rms_{21}^a 8 MHz mK	$I_{\rm CO(1-0)}$ K km s^{-1}	$I_{\rm CO(2-1)}$ K km s^{-1}	$T_{\rm cont,10}$ mK	$T_{\rm cont,21}$ mK
blank sky	11.5	4.2[b]	22.5	9.1	4.2	7.3[b]	.20	.32	2.2 ± 2.5	0 ± 13
NGC 315	15.6	5.0[b]	33.7	12.1[b]	4.7	11.7	.24	.43	102 ± 3.2	47 ± 13
NGC 720	23.8	7.5[b]	60.3	19.6[b]	7.5	19.2	.36	.69	0 ± 9.7	0 ± 43
NGC 4365	11.9	4.6[b]	22.5	7.2[b]	4.3	7.2	.22	.25	0 ± 36	0 ± 80
NGC 4406	17.6	6.0[b]	60.0	20.9[b]	6.0	20.8	.29	.73	0 ± 8.9	17 ± 33
NGC 4472	8.1	2.8[b]	19.6	7.0[b]	2.8	6.8	.13	.25	0 ± 24	29 ± 55
NGC 4636	34.0	9.5[b]	50.5	28.4	9.5	20.1[b]	.45	1.0	37 ± 73	168 ± 140

Notes to Table 2:

rms_{10} and rms_{21} refer to the rms noise in the CO(1–0) and CO(2–1) line observations respectively with no baseline subtraction. The spectral resolution is given in the second row. Noise levels expressed as integrated intensities ($I_{\rm CO}$) have been calculated assuming a 100 km s^{-1} wide line. The last two columns give the continuum temperature measured at the CO(1–0) and CO(2–1) line frequencies. *a*: rms noise after subtraction of a first-order (linear) baseline. *b*: resolution and baseline of spectra shown in Fig. 1.

The half-power beam-widths (HPBW) of the telescope at the frequencies of the ^{12}CO (1–0) and ^{12}CO (2–1) lines are about 22″ and 11″ at 115 and 230 GHz respectively. At the distance of the Virgo cluster (18 Mpc assumed here), this corresponds to roughly 2 and 1 kpc respectively. The pointing was checked at least every 2 hours and the pointing accuracy was $\sim$ 2″ (1 σ). The receivers were aligned to $\sim$ 2″ or better. Two 512 × 1 MHz filter banks were used along with, for some observations, an acousto-optical spectrometer for the second 1.3 mm receiver. All data are presented in the main beam temperature scale and we have assumed efficiencies of η_{115} = 0.6 and η_{230} = 0.45 in all calculations. The nutating secondary was used with a 240″ azimuthal throw and a frequency of 0.25 Hz.

In addition to the source list (Table 1), we have also observed a patch of blank sky in order to check for any low-level instrumental effects. The blank sky observation was reduced in exactly the same way as the sources. No peculiar effects were noticed.

The data were reduced with CLASS software. In the first step, the spectra were checked individually for bad channels. Only one was found, affecting a small number of spectra. We then searched for continuum emission by averaging all channels together in each spectrum and then weighting the average value by the inverse square of the rms noise to calculate the continuum emission (Table 2). The continuum level was then subtracted from each spectrum.

The full-resolution spectra were then averaged and the rms noise calculated. As we present no detections, no channels were left out of the above calculations. Table 2 presents the rms noise values at the full resolution (1 MHz) and smoothed to 8 MHz for the ^{12}CO (1–0) and ^{12}CO (2–1) lines (columns 2-5) with no baseline subtraction. We also tried subtracting a linear baseline from the smoothed spectra and the rms noise values are given in columns 6 and 7 for ^{12}CO (1–0) and ^{12}CO (2–1) respectively. All CO intensities are determined using the limits in columns 3 and 5 [CO(1–0) and CO(2–1), smoothed, no baseline subtraction]. Spectra of all sources are shown in Figure 1 after subtraction of the continuum level.

The integrated intensities in CO (columns 8 and 9) were estimated assuming a line width of 100 km s^{-1}. As no detec-

tions were obtained, no line widths were measured and thus $100\,\mathrm{km\,s^{-1}}$ may not be correct for some or all sources. As long as the line width is small compared to the bandwidth, $I_{\rm CO} \propto I_{\rm CO_{100}}\,(\Delta V/100\,\mathrm{km\,s^{-1}})^{1/2}$.

3. Comments on individual galaxies

3.1. NGC 315

We have detected the continuum emission from NGC 315 at 113.3 GHz and possibly at 226.7 GHz. Heckman et al. (1983) found a 21cm continuum flux density of 1.1 Jy for this extended source. In order to convert our continuum temperature (main beam scale) to a flux density, we multiply $T_{\rm cont}$ by $6.3\,\mathrm{Jy/\,K}\times\eta_{\rm mb}/\eta_{\rm forw}$, yielding a flux density of .42 Jy. A similar calculation gives a flux density of .26 Jy at 1.3 mm. The 21cm to 2.6mm spectral index is then about $-.2$ which is quite flat. The spectral index between 2.6 and 1.3mm is significantly steeper, about -0.7, indicating that either the spectrum steepens with frequency or that the source is $\gtrsim 10''$ at mm wavelengths. If the emission were due to dust, it would be stronger at 1.3 mm.

Despite our non-detection in CO, some cool gas is clearly present in or near NGC 315 as HI is detected in absorption (Heckman et al. 1983; Chamaraux et al. 1987) with $N_{\rm HI} \approx 10^{20}\,\mathrm{cm^{-2}}$.

3.2. NGC 4365

The ^{12}CO (2–1) emission in NGC 4365 nearly reaches the 3σ level but was clearly not detected in CO(1-0) (see Table 2). The ^{12}CO (2–1) "line" is not at the optical velocity of $1227\,\mathrm{km\,s^{-1}}$ but at $v \approx 1115\,\mathrm{km\,s^{-1}}$. NGC 4365 was not detected in HI. We do not consider this to be a CO detection.

3.3. NGC 4406

The detection of HI by Bregman et al. (1988) and the non-detection of CO by us implies that the neutral ISM is strongly dominated by atomic rather than molecular gas. A precise limit cannot be determined because our CO observations only cover the center of the galaxy whereas the HI observations include a much larger region. CO non-detections were also obtained by Lees et al. (1991) and Wiklind et al (1995).

3.4. NGC 4472

CO detections from NGC 4472 have been reported by Huchtmeier et al. (1988, 1994), although their second "detection" is quite different from the first. We observed this position $1'$ South of the nucleus (our data is given for this position) and found no emission at a level well below their reported detections. NGC 4472 was observed during both the May/June run and the August run with non-detections in both cases. We conclude that CO has not been detected in NGC 4472. We also observed the central position for a shorter time and also found nothing (spectrum not shown).

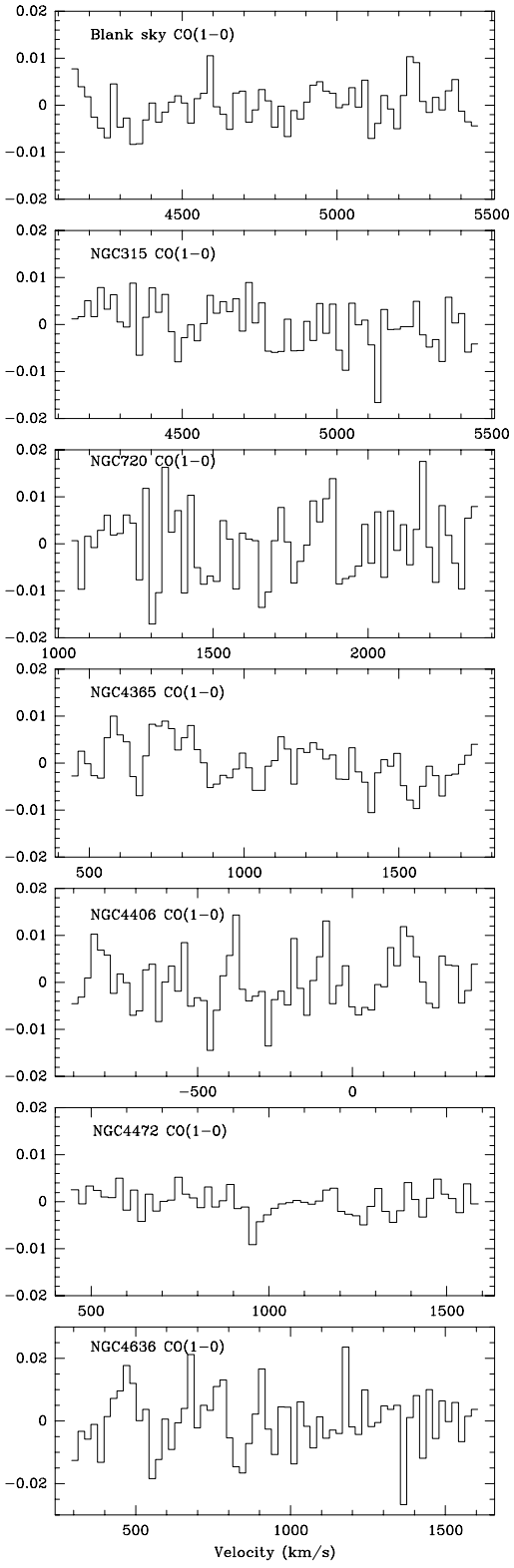

Fig. 1a. Spectra of all galaxies observed in the CO(1–0) line. The y-axis is the antenna temperature in the main-beam scale in Kelvins. The order of the spectra is the same as in Table 2

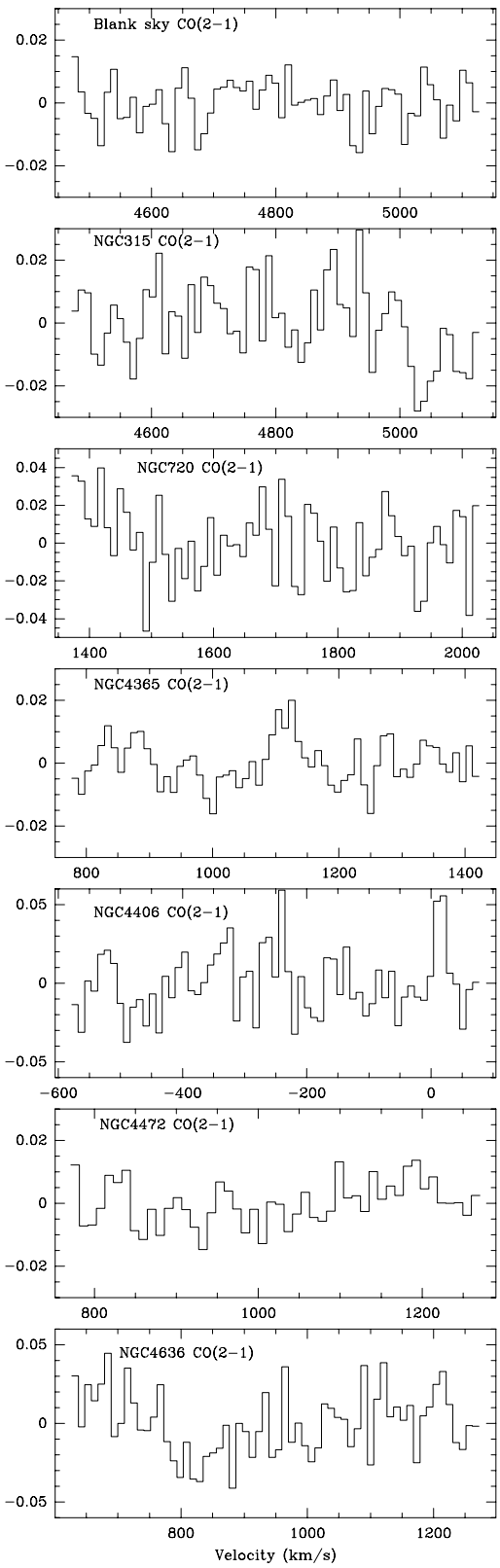

Fig. 1b. Spectra of all galaxies observed in the CO(2–1) line. The y-axis is the antenna temperature in the main-beam scale. The order of the spectra is the same as in Table 2

The most sensitive HI measurements of NGC 4472 have yielded a non-detection (see Huchtmeier & Richter 1989; Roberts et al. 1991; McNamara et al. 1994). The neutral ISM in NGC 4472 is thus very poor indeed.

4. Observed and expected H_2 masses

The goal is to estimate the molecular gas masses (or limits) in the galaxies observed here. We then want to compare the values to what would be expected from cooling flow theory and those obtained from previous observations of other ellipticals. For the comparison with cooling flow theory we focus on the four galaxies which are part of the Thomas et al. (1986) sample. The numbers can be compared directly as we use their assumed distances.

4.1. Molecular gas mass

Cool H_2 is not directly observable. CO is the most readily detected molecule at temperatures typical of the neutral ISM. The conversion of CO intensities to $M_{\rm H_2}$ is a subject of debate, especially for galaxies where the conditions are clearly different from those in the disk of the Milky Way. For both elliptical and spiral galaxies the conversion factors typically applied are $N({\rm H_2})/I_{\rm CO} \lesssim 2\,10^{20}\,{\rm cm^{-2}}/({\rm K\,km\,s^{-1}})$ (*e.g.* Dickman et al. 1986; Combes 1991; O'Dea et al. 1994; Braine et al. 1995; Mauersberger et al. 1996). The metallicity in large elliptical galaxies is at least as high as in spirals so we do not expect to underestimate the amount of molecular gas for lack of C and O. If the temperature of the molecular gas approaches the 2.7 K background radiation, then it will become invisible in emission. The fact that IRAS detected a substantial number of ellipticals at 60 and 100μ means that a "warm" ($\gtrsim 30$ K) dust component is present (Knapp et al. 1989 claim a 45% detection rate for ellipticals with magnitude $m \leq 14$). Wiklind & Henkel (1995) detected 1.2 mm thermal dust emission from most elliptical galaxies in their sample. There is no observational evidence for a very cold ($\lesssim 3$ K) component in the ISM of ellipticals. We assume $N({\rm H_2})/I_{\rm CO} = 2\,10^{20}\,{\rm cm^{-2}}/({\rm K\,km\,s^{-1}})$ for the calculations here.

The molecular gas mass (including the mass of helium contained in the "molecular" clouds) in the telescope beam is thus

$$M_{\rm gas} = 58 \frac{N({\rm H_2})/I_{\rm CO}}{10^{20}}\, D^2_{\rm Mpc}\, \frac{0.73}{f_{\rm H}}\, \theta''^2_{\rm hpbw}\, I_{\rm CO}\ \ {\rm M_\odot} \qquad (1)$$

where f_H is the mass fraction in the form of hydrogen. $N({\rm H_2})/I_{\rm CO}$ is in ${\rm cm^{-2}}$ per ${\rm K\,km\,s^{-1}}$, $I_{\rm CO}$ is in ${\rm K\,km\,s^{-1}}$, and the constant takes care of all the default values and conversion of units.

4.2. $M_{\rm H_2}$ expected from cooling flow scenario

If the hot gas is not reheated and actually cools at the rate suggested by Thomas et al. (1986 or other cooling flow proponents), then it should become molecular at some point after going through an atomic phase (Fabian et al. 1991). Thomas

Table 3. Luminosities, Masses, and mass inflow estimates and limits

Source	L_x 10^6 L$_\odot$	M_x 10^8 M$_\odot$	$\dot{M}_x$ M$_\odot$ yr^{-1}	$L_{\rm B}$ 10^{10} L$_\odot$	$M_{\rm H_2\,10}$ 10^6 M$_\odot$	$M_{\rm H_2\,21}$ 10^6 M$_\odot$	$\dot{M}_{\rm H_2,22''}$ M$_\odot$ yr^{-1}	$\dot{M}_{\rm H_2,11''}$ M$_\odot$ yr^{-1}	$\dot{M}_{x,22'',a}$ M$_\odot$ yr^{-1}	$\dot{M}_{x,22'',b}$ M$_\odot$ yr^{-1}
NGC 315	287	622	2.2	30	140	60	.28	.12	0.5	0.2
NGC 720	49	43	$\gtrsim 0.4$	6.7	24	11	.05	.022		
NGC 4365	5.1	8.3	$\gtrsim 0.04$	4.4	5		.01			
NGC 4406	95	78	> 0.76	8.5	6.4	4	.013	.008	0.02	0.025
NGC 4472	180	178	> 1.5	13	3	1.3	.006	.0026	0.05	0.021
NGC 4636	100	26	> 0.74	3.4	7.5	4	.015	.008	0.09	0.032

Notes to Table 3:

To calculate the X-ray luminosity we have assumed, as is appropriate for a gas at around 1 keV, that $L_x = L_{.5-4.5}/0.6$ where $L_{.5-4.5}$ is determined as in equation 4 of Roberts et al. (1991). L_x for NGC 315 is from Forman et al. (1985). M_x is the mass of hot gas and has been calculated using Eq. (4) of Roberts et al. (1991). $\dot{M}_x$ is from Thomas et al. (1986) taken to be the average of their methods i and ii (typical difference is $\sim$30%). For NGC 720 and 4365 we based our estimate of $\dot{M}_x$ on the average $L_x/\dot{M}_x$ value for the other four galaxies. Blue luminosities are calculated using $M_{\rm B_\odot} = 5.48$. $M_{\rm H_2\,10}$ and $M_{\rm H_2\,21}$ are the noise levels expressed in terms of the H_2 mass as calculated in Sect. 4.1 for the CO(1–0) and CO(2–1) lines. No value is given for $M_{\rm H_2\,21}$ in NGC 4365 because of a peak near 3σ. $\dot{M}_{\rm H_2,22''}$ and $\dot{M}_{\rm H_2,11''}$ are the noise levels expressed in terms of a mass inflow rate for the CO(1–0) and CO(2–1) beams (see Section 4.2). $\dot{M}_{x,22'',a}$ and $\dot{M}_{x,22'',b}$ are the $\dot{M}_x$ expected within the ^{12}CO beam. The first is calculated by extending the curves given in Thomas et al.'s Fig. 4 to the size of the ^{12}CO beam. The second is by assuming that $\dot{M}_x(r < R) \propto R$ (cf. Fabian et al. 1991) and using the cooling radius given in Thomas et al.'s Table 3.

et al. (1986) use two methods to determine the inflow rate $\dot{M}_x$ which only differ by 30–40%. We give the average value in Table 3. The "cooling region" is typically an order of magnitude larger than our CO(1–0) beam so direct comparison is not appropriate. We estimate $\dot{M}_x$ within our telescope beam by (a) extending the curves in Figure 4 of Thomas et al. to the radius of our beam and (b) by assuming that $\dot{M}_x(r < R) \propto R$ (Fabian et al. 1991). These values are given in Table 3.

Using the same logic as Grabelsky & Ulmer (1990) and Braine & Dupraz (1994), if there is a steady-state (*i.e.* long-lived) inflow of gas, then the inflow equals the outflow of mass (presumably to star formation) and the mass in a given phase is equal to the time spent by a unit of matter in the phase (years) multiplied by the mass per year being turned into (or out of) the phase (M$_\odot$ yr^{-1}):

$$M_{\rm phase} = \langle \tau_{\rm transformation} \rangle \times \dot{M} \ . \quad (2)$$

If molecular gas is forming from the hot gas observed in the X-ray band, we expect to find roughly $M_{\rm H_2} = \tau_{\rm SF} \dot{M}_x / {\rm M}_\odot$, where $\tau_{\rm SF}$ is the average time required to transform molecular gas completely into stars (or substellar masses). No observational evidence exists for an average $\tau_{\rm SF}$ approaching the free-fall time of molecular clouds. In order to estimate $\tau_{\rm SF}$ we need data enabling us to estimate the ratio of the star formation rate $\dot{M}$ and $M_{\rm H_2}$, preferably for elliptical galaxies. Imperfect but well-known and widely discussed tracers are the FIR luminosity for $\dot{M}_{\rm SF}$ and the CO luminosity for $M_{\rm H_2}$. Assuming that $\dot{M}_{\rm SF} \approx 1\,{\rm M}_\odot\,{\rm yr}^{-1}$ when $L_{\rm FIR} \approx 10^{10}\,{\rm L}_\odot$, one can use the $L_{\rm FIR}$ vs. $M_{\rm H_2}$ diagram in Wiklind et al. (1995) to estimate $\tau_{\rm transformation}$. One obtains $\tau_{\rm transformation} = \tau_{\rm SF} \approx 5\,10^8$ yr for elliptical galaxies.

It should be emphasized that $\tau_{\rm transformation}$ (or $\tau_{\rm SF}$) is *not* a cloud lifetime. In a molecular cloud, some dense cores collapse to form stars and this disperses most of the remaining material. Thus, most hydrogen atoms do not form stars during the nominal collapse time of a cloud but may be dispersed several times before becoming part of a star. This is why $\tau_{\rm transformation}$ (or $\tau_{\rm SF}$) is significantly greater than the lifetime of a cloud.

Looking at the above expressions for the "observed" $M_{\rm H_2,CO}$ and the "expected" $M_{{\rm H_2},x}$ (expected from cooling flow theory), it is apparent that the ratio $M_{{\rm H_2},x}/M_{\rm H_2,CO}$ is independent of the $N({\rm H_2})/I_{\rm CO}$ value used as long as the ellipticals observed here are not highly unrepresentative. Thus,

$$\frac{M_{{\rm H_2},x}}{M_{\rm H_2,CO}} = \frac{\dot{M}_x}{L_{\rm CO}} \left\langle \frac{L_{\rm CO}}{\dot{M}_{\rm SF}} \right\rangle_{\rm ell} . \quad (3)$$

Let us recall that Thomas et al. found the "cooling flow " phenomenon in each galaxy in their sample. If the ratio above is less than unity (and CO detected), then an additional source for the gas is necessary. If greater than unity, as is the case here, then less gas than expected reaches the molecular phase.

4.3. Are the observations compatible with cooling flows in elliptical galaxies?

As can be seen by comparing the last columns in Table 3, it is surprising that we have no detections given that the "expected" $M_{\rm H_2}$ values regularly exceed the noise levels. The basic lack of observed neutral gas in cooling flows suggests the inflow rates may be overestimated, most likely due to the presence of a heating source (Faber & Gallagher 1976; Forman et al. 1985). Nonetheless, our non-detections do *not* allow us to clearly rule out the reported inflow rates in these galaxies, principally because of the uncertainties in line widths, conversion from $L_{\rm FIR}$ to a star formation rate, and the transformation time from H_2 to stars.

4.4. Galactic and cluster cooling flows

How does the situation in X-ray bright galaxies compare with cooling flows in clusters?

Despite the fact that galaxies in the centers of bright X-ray clusters have properties similar to those of the ellipticals investigated here, the astrophysical questions and situation are very different.

— the baryonic mass in galaxy clusters appears dominated by the gas while the opposite is true even in X-ray bright ellipticals which are not at the core of a cluster cooling flow.

— the inflow rates are different by 1 - 3 orders of magnitude. Thus, even over a Hubble time, the reported inflow rates for elliptical galaxies could not be responsible for the dark matter in the galaxy. In clusters, the reported mass inflow rates are so high that the dark matter in the inner region of the cluster could be due to a long-lived cooling flow.

— the intracluster gas is several times warmer than the X-ray gas in ellipticals, where supernovae and other heating mechanisms may contribute significantly to the energy balance of the gas.

5. Conclusions

We present new CO(1–0) and CO(2–1) observations of a sample of 6 X-ray bright elliptical galaxies. None of the galaxies were detected by us in CO(1–0) or CO(2–1). Unless our sample is peculiar in some way, X-ray bright ellipticals do not emit strongly in the CO lines. While our limits to the molecular gas mass are not strict enough to clearly rule out all cooling flow scenarios, they suggest that models which do not include heating sources may overestimate the inflow rates. Our data, along with existing HI and CO data for cluster cooling flows, provide no support for the conversion of large masses of hot gas to neutral gas as predicted by standard cooling flow theory.

References

Braine, J., Dupraz, C. 1994, A&A 283, 407.
Braine, J. & Wiklind, T. 1993, A&A 267, L47.
Braine, J., Wyrowski, F., Radford, S.J.E., Henkel, C., Lesch, H. 1995, A&A 293, 315
Bregman, J.N., Roberts, M.S., Giovanelli, R. 1988, ApJ 330, L93.
Caldwell, N. 1984, PASP 96, 287.
Chamaraux, P., Balkowski, C., Fontanelli, P. 1987, A&AS 69, 263.
Combes F. 1991, ARAA 29, 195
Dickman, R.L., Snell, R.L., Schloerb, F.P. 1986, ApJ 309, 326
Draine, B.T., Salpeter, E.E. 1979, ApJ 231, 77.
Elmegreen, B.G. 1985, Protostars & Planets II, eds. D.C. Black, M.S. Matthews, p33.
Faber, S.M., Gallagher, J.S. 1976, ApJ 204, 365
Fabian, A.C., Nulson, P.E.J., Canizares, C.R. 1991, AAR 2, 191
Ferland, G.J., Fabian, A.C., Johnstone, R.M. 1994, MNRAS 266, 399.
Forman, W., Jones, C., Tucker, W. 1985 ApJ 293, 102.
Grabelsky, D.A. & Ulmer, M.P. 1990, ApJ 355, 401.
Heckman, T.M., Balick, B., Van Breugel, W.J.M., Miley, G.K. 1983, AJ 88, 583.
Hill, J.K., Hollenbach, D.J. 1976, ApJ 209, 445
Huchtmeier, W., Bregman, J.N., Hogg, D.E., Roberts, M.S. 1988, A&A 198, L17.
Huchtmeier, W. K., Richter, O.-G. 1989, A General Catalog of H I Observations of Galaxies (New York: Springer-Verlag).
Huchtmeier, W., Bregman, J.N., Hogg, D.E., Roberts, M.S. 1994, A&A 281, 327.
Jura, M., Kim, D.W., Knapp, G.R., Guhathakurta, P. 1987, ApJ 312, L11.
Knapp, G.R., Guhathakurta, P., Kim, D.W., Jura, M. 1989, ApJS 70, 329.
Lazareff, B., Castets, A., Kim, D.-W., Jura, M. 1989, ApJ 335, L13
Lees, J.F., Knapp, G.R., Rupen, M.P., Phillips, T.G., 1991, ApJ 379, 177
Lequeux, J., Viallefond, F. 1980, A&A91, 269
Mauersberger, R., Henkel, C., Wielebinski, R., Wiklind, T., Reuter, H.-P., 1996, A&A 305, 421
McNamara B.R., Jaffe, W. 1994, A&A 281, 673
McNamara B.R., Sancisi, R., Henning, P.A., Junor, W. 1994, A&A 281, 673
Mushotsky, R.F., Loewenstein, M., Awaki, H. et al. 1994, ApJ 436, L79.
O'Dea, C.P., Baum, S.A., Maloney, P.R., Tacconi, L.J., Sparks, W.B. 1994, ApJ 422, 467.
Phillips, M.M., Jenkins, C.R., Dopita, M.A. et al. 1986, AJ 91, 1062.
Roberts, M.S., Hogg, D.E., Bregman, J.N. et al. 1991, ApJS 75, 751.
Sarazin, C.L. 1990, The Interstellar Medium in Galaxies, eds. H.A. Thronson, J.M. Shull, p201.
Spitzer, L. Jr. 1978, *Physical Processes in the Interstellar Medium*, Wiley Interscience, New York.
Thomas, P.A., Fabian, A.C., Arnaud, K.A., Forman, W., Jones, C. 1986, MNRAS 222, 655
de Vaucouleurs, G., de Vaucouleurs, A., Corwin, H.G. et al. 1991, Third Reference Catalog of Bright Galaxies (New York: Springer-Verlag). (RC3)
White, D.A., Fabian, A., Forman, W., Jones, C., Stern, C. 1991, ApJ 375, 35
Wiklind, T., Henkel, C., 1995, A&A, 297, L71
Wiklind, T., Combes, F., Henkel, C., 1995, A&A, 297, 643

This article was processed by the author using Springer-Verlag LaTeX A&A style file *L-AA* version 3.